Dynamical local-field factors and effective interactions in the two-dimensional electron liquid

G. S. Atwal,[1] I. G. Khalil,[2] and N. W. Ashcroft[1]
[1]*Cornell Center for Materials Research, and the Laboratory of Atomic and Solid State Physics, Cornell University, Ithaca, New York 14853-2501*
[2]*Gene Network Sciences, Inc., Ithaca, New York 14853-1509*

(Received 10 October 2002; revised manuscript received 10 January 2003; published 12 March 2003)

We present an analytical study of the dynamical local-field factors associated with the response of a homogeneous two-dimensional interacting electron liquid as functions of momentum, frequency, and density. We derive sum rules that constrain their asymptotic forms (in momentum and frequency) for both the spin-symmetric and spin-antisymmetric cases. Parametrized expressions for the local-field factors are proposed, based on all available sum rules and on many-body perturbation theory, and these are found to be in good agreement with quantum Monte Carlo calculations. Finally, these expressions are used to evaluate the effective electron-electron interaction in a local approximation for two-dimensional systems. It is shown that both the quantitative and qualitative behaviors of the interaction are sensitive to the inclusion of dynamical correlations.

DOI: 10.1103/PhysRevB.67.115107 PACS number(s): 71.45.Gm, 71.10.−w, 71.10.Pm

I. INTRODUCTION

The theoretical study of interacting electron systems in two dimensions, where dynamical correlation effects are strong, continues as a formidable challenge. A useful approach to describing the many-body effects of exchange and correlation (xc) in the dynamic response $\Pi(q,\omega)$ of interacting electron liquids is via the use of local-field factors[1,2] $G(q,\omega)$. For the proper spin-symmetric (s) and spin-antisymmetric (a) responses they may be defined through the statements

$$\Pi^{s,a}(q,\omega)=\frac{\overline{\Pi}_0(q,\omega)}{1+v_q G_{s,a}(q,\omega)\overline{\Pi}_0(q,\omega)}. \tag{1}$$

Here, $v_q=2\pi e^2/q$ is the Fourier-transformed two-dimensional Coulomb potential and the overbar signifies the fact that we must use the modified form of the Lindhard function,[3] $\Pi_0(q,\omega)$, which uses the *exact* occupation numbers, these giving rise to a further local-field factor defined by[4]

$$\overline{\Pi}_0(q,\omega)=\frac{\Pi_0(q,\omega)}{1+v_q G_n(q,\omega)\Pi_0(q,\omega)}. \tag{2}$$

Alternatively, the response functions can be expressed in terms of the bare Lindhard function,

$$\Pi^{s,a}(q,\omega)=\frac{\Pi_0(q,\omega)}{1+v_q \overline{G}_{s,a}(q,\omega)\Pi_0(q,\omega)}, \tag{3}$$

in which case we must have

$$\overline{G}_{s,a}(q,\omega)=G_{s,a}(q,\omega)+G_n(q,\omega). \tag{4}$$

Physically, the local-field factors represent the deviation of the actual response functions (i.e., the full many-body problem) away from the random phase approximation (RPA). Determination of these factors is a fundamental problem of many-body theory, and as yet, it is necessary to resort to some form of approximation. The most widely used and earliest of such approximations[1,5] address the static case which is then also implemented in the dynamical response functions, resulting in a double approximation of the dynamical local-field factors, i.e., $G(q,\omega)\approx G_{\text{approx}}(q)$. However, in the dynamical case, the exchange-correlation hole fluctuates in time and so the local-field factors must also exhibit frequency dependence,[6] more so in two dimensions than in three. It is the purpose of this paper to determine approximate forms of such dynamical local-field factors in homogeneous two-dimensional systems for all **q** and (imaginary) ω in a manner similar to the work of Richardson and Ashcroft[4] who reported results in three dimensions. Working with imaginary frequencies not only simplifies the numerical work, circumventing the singularities along the real frequency axis, but is also a useful framework in which to carry out many subsequent calculations of the electron liquid.

A number of exact results are known about the limiting forms of the local-field factors, and the associated sum rules are thus useful in constraining approximate theories. For example, $\overline{G}_s(q\to 0,\omega=0)$ is given by the compressibility sum rule and $G_s(q,\omega\to\infty)$ is given by the third-moment sum rule. On the other hand, the response functions, as given by second-order perturbation theory, have a singular structure at $q=1$ (units of $2k_F$), a region not accessible by known sum rules. Thus, to determine the quantitative structure at $q=1$ we appeal to a summation of classes of infinite numbers of diagrams within perturbation theory. Guided by both the sum rules and perturbation theory, we derive relatively simple parametrized forms of the local-field factors which we will then show to agree rather well with the results from quantum Monte Carlo (QMC) simulations, currently available only in the static case. However, we find that the singular structure at $q=1$ is less convincingly supported by the QMC data in the spin-symmetric case, demonstrating that perturbation theory to second order may be insufficient to accurately describe the two-dimensional spin-symmetric response at intermediate wave vectors.

Knowledge of the charge and spin responses in an electron liquid is an essential input into determination of the

 ©2003 The American Physical Society

effective interaction between any two electrons within the liquid. Kukkonen and Overhauser[7] (KO) have derived an expression for the effective electron-electron interaction in an homogeneous electron liquid, in which all the xc effects of the medium of interacting electrons are treated in a local approximation. This permits the effective interaction to be expressed in terms of the local-field factors that act to renormalize the direct Coulomb potential. Both spin-symmetric and spin-antisymmetric local-field factors are required to include direct and exchange contributions in a consistent manner. We rewrite the KO expression, using the modified form of the Lindhard function, to emphasize the need to include self-energy effects properly to determine the correct behavior at large **q**. The evaluation of the resulting modified KO expression then requires G_s, G_a, and G_n as input.

The plan of this paper is as follows. In Sec. II we derive the parametrized forms of the local-field factors by first carrying out a perturbative analysis via the diagrammatic route and then later considering all the sum rule constraints. In Sec. III we compute the effective electron-electron interaction and in Sec. IV we end with some conclusions.

II. TWO-DIMENSIONAL LOCAL-FIELD FACTORS

A. Perturbative calculations

The techniques we employ to solve the integral equations for the spin-symmetric and spin-antisymmetric vertex functions are detailed in Ref. 4 and Ref. 8, and here we simply outline the main steps and introduce the notation. The integral equations for the electron-electron vertex function that include the lowest order effects of exchange and correlation are given by [see Fig. 1 of Ref. 4],

$$\begin{aligned}\Lambda^{s,a}(\tilde{p},\tilde{q}) = 1 &- \mathrm{Tr}_{\tilde{p}'}[v_{\mathrm{RPA}}(\tilde{p}-\tilde{p}') + \Gamma^{s,a}(\tilde{p},\tilde{p}';\tilde{q})] \\ &\times G_0(\tilde{p}'+\tilde{q})G_0(\tilde{p}')\Lambda^{s,a}(\tilde{p}',\tilde{q}) \\ &- \Lambda^{s,a}(\tilde{p},\tilde{q})\mathrm{Tr}_{\tilde{p}'}[G_0(\tilde{p}+\tilde{q})G_0(\tilde{p}'+\tilde{q}) \\ &+ G_0(\tilde{p})G_0(\tilde{p}')v_{\mathrm{RPA}}(\tilde{p}'-\tilde{p})], \end{aligned} \tag{5}$$

where the superscript denotes symmetric (s) or antisymmetric, (a) $\tilde{p}=(i\omega_p,\mathbf{p})$, $\mathrm{Tr}_{\tilde{p}}$ denotes the trace over all frequency and momenta, i.e., $\int d\omega_p \int d^2p/(2\pi)^2$, G_0 is the noninteracting Green's function,

$$\begin{aligned}\Gamma^{s}(\tilde{p},\tilde{p}';\tilde{q}) = \mathrm{Tr}_{\tilde{k}} &v_{\mathrm{RPA}}(\tilde{k})v_{\mathrm{RPA}}(\tilde{k}+\tilde{q})G_0(\tilde{k}-\tilde{p}) \\ &\times[G_0(\tilde{p}'-\tilde{k}) + G_0(\tilde{k}+\tilde{p}'+\tilde{q})], \end{aligned} \tag{6}$$

and finally

$$\Gamma^{a}(\tilde{p},\tilde{p}';\tilde{q}) = 0. \tag{7}$$

All momenta are expressed in units of $2k_F$ and all energies in units of $2k_F^2/m$, ($\hbar=1$). Note that the Coulombic interaction in Eq. (5) is screened within the standard RPA, i.e.,

$$v_{\mathrm{RPA}}(\tilde{q}) = v_q/[1-v_q\Pi_0(\tilde{q})]. \tag{8}$$

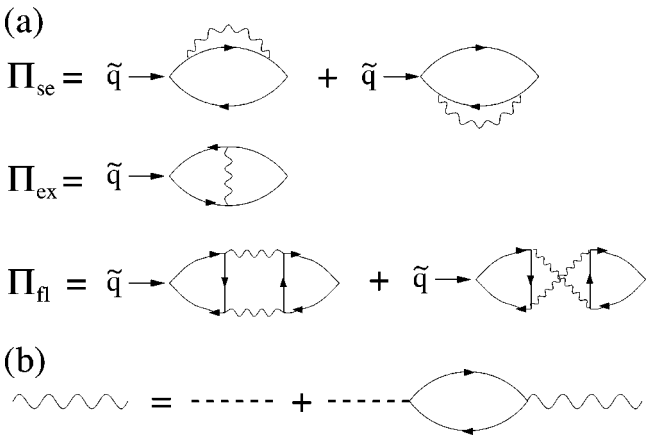

FIG. 1. Leading-order contributions to the proper polarizability function. (a) Diagrammatic representation of polarization bubbles arising from self-energy, exchange, and fluctuations. (b) Dyson equation for the screened potential (RPA).

By means of a variational approach,[9] we can implement the following trial solution with $\Lambda^{s,a}(\tilde{p},\tilde{q})=\Lambda^{s,a}(\tilde{q})$ representing a local approximation, and we can also express the vertex functions in terms of polarizability functions, thus

$$\Lambda^{s}(\tilde{q}) = \frac{\Pi_0(\tilde{q})}{\Pi_0(\tilde{q})-\Pi_{\mathrm{se}}(\tilde{q})-\Pi_{\mathrm{ex}}(\tilde{q})-\Pi_{\mathrm{fl}}(\tilde{q})}, \tag{9}$$

and

$$\Lambda^{a}(\tilde{q}) = \frac{\Pi_0(\tilde{q})}{\Pi_0(\tilde{q})-\Pi_{\mathrm{se}}(\tilde{q})-\Pi_{\mathrm{ex}}(\tilde{q})}, \tag{10}$$

where the leading-order contributions to the expansion of the polarizability function are shown in Fig. 1. The self-consistent choice of diagrams is dictated by the requirement of gauge invariance or, equivalently, by the application of Ward-Pitaevskii identities,[10] thereby ensuring that conservation laws are enforced in the electron dynamics.[11] As previously noted,[8,12,13] the polarizability diagrams in Fig. 1 can all be expressed in terms of the three-point function $\Lambda^{(3)}(\tilde{q},\tilde{p})$; thus

$$\begin{aligned}\Pi_{\mathrm{se}}(\tilde{p}) = \mathrm{Tr}_{\tilde{q}} &v_{\mathrm{RPA}}(\tilde{q})\left[\frac{\partial}{\partial(i\omega_q)} - \frac{\partial}{\partial(i\omega_p)}\right] \\ &\times[\Lambda^{(3)}(\tilde{p},qt) + \Lambda^{(3)}(\tilde{q},\tilde{p})], \end{aligned} \tag{11}$$

$$\begin{aligned}\Pi_{\mathrm{ex}}(\tilde{p}) = \mathrm{Tr}_{\tilde{q}} &\frac{v_{\mathrm{RPA}}(\tilde{q})}{\mathbf{p}\cdot\mathbf{q}}[\Lambda^{(3)}(\tilde{p},\tilde{q}) + \Lambda^{(3)}(\tilde{q},\tilde{p}) \\ &- \Lambda^{(3)}(-\tilde{p},\tilde{q}) - \Lambda^{(3)}(\tilde{q},-\tilde{p})], \end{aligned} \tag{12}$$

$$\begin{aligned}\Pi_{\mathrm{fl}}(\tilde{p}) = -\frac{1}{2}&\mathrm{Tr}_{\tilde{q}} v_{\mathrm{RPA}}(\tilde{q})v_{\mathrm{RPA}}(\tilde{p}-\tilde{q}) \\ &\times[\Lambda^{(3)}(\tilde{q},\tilde{p}-\tilde{q}) + \Lambda^{(3)}(\tilde{p}-\tilde{q},\tilde{q})]^2. \end{aligned} \tag{13}$$

An explicit formula for the three-point function $\Lambda^{(3)}(\tilde{p},\tilde{q})$ in two dimensions has been given by Neumayr and Metzner.[14]

To make connection with the local-field factors it is necessary to isolate the first-order correction to the modified Lindhard function,

$$\overline{\Pi}_0^{(1)}(\tilde{q})=\Pi_0(\tilde{q})+\Pi_{\rm se}(\tilde{q})-\overline{\Pi}_{\rm se}(\tilde{q}), \tag{14}$$

where

$$\overline{\Pi}_{\rm se}(\tilde{q})=\frac{2m}{k_f^2}{\rm ReTr}\frac{G_0(\tilde{k})[\Sigma_{RPA}(\tilde{k}+\tilde{q})-\Sigma_{RPA}(\tilde{k})]}{(i\omega_q-q^2-2\mathbf{k}\cdot\mathbf{q})^2}, \tag{15}$$

is the number-renormalized self-energy contribution to the polarizability [cf. $\Pi_{\rm se}(\tilde{q})$ that incorporates the free Fermi gas occupation numbers]. Here $\Sigma_{\rm RPA}(\tilde{k})$ is the electron self-energy in the RPA.

The local-field factors are then given by

$$G_s(\tilde{q})=\frac{-1}{v_q\Pi_0^2(\tilde{q})}[\overline{\Pi}_{\rm se}(\tilde{q})+\Pi_{\rm ex}(\tilde{q})+\Pi_{\rm fl}(\tilde{q})], \tag{16}$$

$$G_a(\tilde{q})=\frac{-1}{v_q\Pi_0^2(\tilde{q})}[\overline{\Pi}_{\rm se}(\tilde{q})+\Pi_{\rm ex}(\tilde{q})], \tag{17}$$

and

$$G_n(\tilde{q})=\frac{-1}{v_q\Pi_0^2(\tilde{q})}[\overline{\Pi}_0^{(1)}(\tilde{q})-\Pi_0(\tilde{q})]. \tag{18}$$

The results of the numerical calculations have been partially reported elsewhere[8,15] and it has been noted that for the two-dimensional electron liquid the inclusion of fluctuation diagrams provides significant enhancement to the proper polarizability function.

A shortcoming of the perturbative method is that, in addition to the increasing inaccuracy at higher r_s, the calculated local-field factors diverge at large q and thus do not obey the known large q sum rules that predict finite asymptotic values. In the following section we discuss the sum-rule constraints that will then later be used, in conjunction with the numerical results from Eqs. (16)–(18) at low q, to determine simple parametrized expressions for the local-field factors.

B. Constraints

In the static limit, $\omega=0$, all local-field factors are linear in q in the limit of small q, i.e.,

$$\lim_{q\to 0}G_i(q,0)=\lambda_i^0(r_s)q \quad (i=s,a,n). \tag{19}$$

The combination $\lambda_s^0(r_s)+\lambda_n^0(r_s)$ is determined from the compressibility sum rule,

$$\lambda_s^0(r_s)+\lambda_n^0(r_s)=\frac{2}{\pi}+\frac{r_s^2}{2^{5/2}}\frac{\partial\epsilon_c(r_s)}{\partial r_s}-\frac{r_s^3}{2^{5/2}}\frac{\partial^2\epsilon_c(r_s)}{\partial r_s^2}, \tag{20}$$

where $\epsilon_c(r_s)$ is the correlation energy per particle (expressed in units of Rydbergs) which can be extracted from Monte Carlo simulations.[16] The combination $\lambda_a^0(r_s)+\lambda_n^0(r_s)$ is determined from the spin susceptibility,

$$\lambda_a^0(r_s)+\lambda_n^0(r_s)=\frac{2}{\pi}-\frac{r_s}{2^{1/2}}\frac{\partial^2\epsilon_c(\xi)}{\partial\xi^2}, \tag{21}$$

where ξ is the spin polarization. Another constraint is required to separately determine λ_n^0 and for this we appeal to the perturbative calculations, where we find that

$$\frac{\lambda_n^0(r_s)}{\lambda_a^0(r_s)}\approx-\frac{r_s}{10+5r_s} \tag{22}$$

provides a reasonable approximation for the ratio of the gradients of the respective local-field factors at $q=0$ for $1\leqslant r_s\leqslant 10$. Note that, other than the fact that we chose to match the Richardson-Ashcroft[4] formalism as much as possible, there is no *a priori* reason why the fitting formula Eq. (22) should take the proposed form. However, some justification for retaining this form is provided *ex post facto* by the good agreement with QMC data, as will be demonstrated in the following section.

In the determination of the dynamic local-field factors it has been overlooked in some previous work that at very long wavelengths the low-ω limit does not correspond to the static limit as given above,[17] i.e., $\lim_{\omega\to 0}\lim_{q\to 0}\neq\lim_{q\to 0}\lim_{\omega\to 0}$. Mathematically this behavior stems from the singular value of the vertex function $\Lambda(q,\omega)$ at the origin. A more physical explanation can be seen in the work of Conti and Vignale[18] who derived $\lim_{\omega\to 0}\lim_{q\to 0}G(q,i\omega)=E_F/(2v_q)[(F_2-3F_1+4F_0)/(F_1+2)]$ where F_l are the Landau parameters. From the available QMC calculations[19] of the Landau parameters we find that this expression differs from Eq. (19) by 3% at $r_s=1$ and 4% at $r_s=5$, and hence, for the sake of simplicity, we choose not to take this minor difference into account.

We turn our attention to further constraints on G_s and G_a. The large ω limit of G_s and G_a is determined by the third-moment sum rule,[20,21] which in the low q limit is given by

$$\lim_{q\to 0}\lim_{\omega\to\infty}G_s(q,i\omega)=\lambda_s^\infty(r_s)q, \tag{23}$$

and by

$$\lim_{q\to 0}\lim_{\omega\to\infty}G_a(q,i\omega)=\lambda_a^\infty(r_s)/q. \tag{24}$$

Here

$$\lambda_s^\infty(r_s)=\frac{5}{3\pi}+\frac{7}{2^{5/2}}r_s\epsilon_c(r_s)+\frac{19}{2^{7/2}}r_s^2\frac{\partial\epsilon_c(r_s)}{\partial r_s}, \tag{25}$$

and

$$\lambda_a^\infty(r_s)=2\int_0^\infty dk k^2[\tilde{S}(k)-S(k)], \tag{26}$$

where $\tilde{S}(k)$ is the antisymmetric structure factor and $S(k)$ is the symmetric structure factor (Sec. II C). The large ω limit of G_n follows from an appropriate expansion of the expression for the modified Lindhard function, namely,

$$\lim_{\omega\to\infty}\overline{\Pi}_0(q,i\omega)=\lim_{\omega\to\infty}\Pi_0(q,i\omega)+\frac{3mq^4}{\pi\omega^4}(\langle E_{KE}\rangle-\langle E_{KE}\rangle_0), \tag{27}$$

giving[21]

$$\lim_{q\to 0}\lim_{\omega\to\infty}G_n(q,i\omega)=\lambda_n^\infty(r_s)q, \tag{28}$$

where

$$\lambda_n^\infty(r_s)=\frac{3r_s}{2^{1/2}}\frac{\partial}{\partial r_s}[r_s\epsilon_c(r_s)]. \tag{29}$$

In the last line we have applied the generalized virial theorem.[2] The large q limits of G_s and G_a turn out to be frequency-independent (in contrast to the equivalent three-dimensional results) and have been evaluated to be[22]

$$\lim_{q\to\infty}G_s(q,i\omega)=1-g(0) \tag{30}$$

and

$$\lim_{q\to\infty}G_a(q,i\omega)=g(0), \tag{31}$$

where $g(0)$ is the electron pair correlation function evaluated at the origin. In addition, a large q expansion of the modified Lindhard integral gives the asymptotic behavior of G_n, namely,

$$\lim_{q\to\infty}G_n(q,i\omega)=-\frac{r_sq}{2^{1/2}}\frac{d}{dr_s}[r_s\epsilon_c(r_s)]=-\frac{\lambda_n^\infty}{3}q. \tag{32}$$

At intermediate wave vectors there are extrema in G_i: in the static case ($\omega=0$) the peaks occur at $q=1$ arising from the singular nature of the response at this value of q. We find that the perturbative results, at low q and high r_s, are well approximated by taking

$$G_i(q=1,0)\approx\zeta_i\lambda_i^0(r_s)\quad(i=s,a,n), \tag{33}$$

where $\zeta_s=1.4$, $\zeta_a=0.9$, and $\zeta_n=1.0$. Since the numerical local-field factors are nonlinear in the region $0<q<1$, Eq. (33) notably underestimates the peak heights near $q=1$. However, the error in the combined local-field factors Eq. (4) is reduced somewhat by the opposing signs of G_n and $G_{s,a}$ in this region. The comments made just after Eq. (22) also apply here for retaining the form of Eq. (33).

In the large ω limit the peaks occur at $\omega=q^2$, as can be seen by differentiation of the the expression of the local field factors in this limit,[23,24] i.e.,

$$\lim_{\omega\to\infty}G_{s,a}(q,i\omega)=\frac{1}{2N}\sum_{q'}\sum_{\sigma,\sigma'}\left[\alpha(q,\omega)\frac{(\mathbf{q}\cdot\mathbf{q}')^2v_{\mathbf{q}'}}{q^4v_{\mathbf{q}}}-\eta_{s,a}(\sigma,\sigma')\frac{[\mathbf{q}\cdot(\mathbf{q}+\mathbf{q}')]^2v_{\mathbf{q}+\mathbf{q}'}}{q^4v_{\mathbf{q}}}\right]\times[S_{\sigma,\sigma'}(q')-\delta_{\sigma\sigma'}], \tag{34}$$

where $\eta_s(\sigma,\sigma')=1$, $\eta_a(\sigma,\sigma')=\mathrm{sgn}(\sigma\sigma')$, and

$$\alpha(q,\omega)=\frac{(i\omega+q^2)^4+(i\omega-q^2)^4}{2(\omega^2+q^4)^2}. \tag{35}$$

These peak values are found to be identical to those given in Eq. (30) and Eq. (31). From Eq. (27) it is possible to show that $G_n(q,i\omega)$ has a minimum at $q^2=\omega/\sqrt{7}=0.38\omega$ with the peak height given by

$$G_n(q=q_{\min},i\omega)=1.304\omega^{1/2}r_s\frac{d}{dr_s}[r_s\epsilon_c(r_s)], \tag{36}$$

again, in the large ω limit.

C. Parametrization

To obtain expressions for the parametrized forms of the local-field factors, we must specify, in addition to the above constraints, where the extrema lie as functions of all q and ω. We interpolate between the location of the extrema at the static regime and the high-frequency regime as follows: the maxima of G_s and G_a are taken to be located at $q^2=1+\omega$ and the minima of G_n is taken to be located at $q^2=1+0.38\omega$.

1. $G_s(q,i\omega)$

Guided by the sum rules, we parametrize the dynamical spin-symmetric local field factor as a rational fraction, polynomial in q and with ω-dependent coefficients,

$$G_s(q,i\omega)=\frac{a_s(\omega)q+b_s(\omega)q^7}{1+c_s(\omega)q+d_s(\omega)q^7}, \tag{37}$$

where the coefficients are constrained to be

$$a_s(\omega)=\frac{\lambda_s^0+\omega^2\lambda_s^\infty}{1+\omega^2}, \tag{38}$$

$$b_s(\omega)=d_s(\omega)[1-g(0)], \tag{39}$$

$$c_s(\omega)=\frac{a_s(\omega)}{1-g(0)}-\frac{7}{6(1+\omega)^{1/2}}-\frac{a_s(\omega)}{6b_s(\omega)(1+\omega)^{7/2}}, \tag{40}$$

and

$$d_s(\omega)=\frac{\zeta_s}{6[\zeta_s-1+g(0)](1+\omega^4)}-\frac{\lambda_s^\infty\omega}{[1-g(0)](1+\omega^4)}. \tag{41}$$

The polynomials are simply chosen to be of the lowest orders such that not only are sum rules satisfied but also that root solutions in the denominator are obviated. The expression for $c_s(\omega)$ follows from the condition that the maxima be located at $q^2=1+\omega$.

2. $G_a(q,i\omega)$

In a similar way, the spin-antisymmetric local-field factor is parametrized as

$$G_a(q,i\omega)=\frac{a_a(\omega)q^{-1}+b_a(\omega)q+c_a(\omega)q^7}{1+d(\omega)q+e(\omega)q^7}, \tag{42}$$

where

$$a_a(\omega)=\frac{\lambda_a^\infty\omega^2}{1+\omega^2}, \tag{43}$$

$$b_a(\omega)=\frac{\lambda_a^0}{1+\omega^2}, \tag{44}$$

$$c_a(\omega)=e_a(\omega)g(0), \tag{45}$$

$$d_a(\omega)=\frac{a_a(\omega)[8e_a(\omega)(1+\omega)^{7/2}+1]+b_a(\omega)[6e_a(\omega)(1+\omega)^{9/2}-1+\omega]-7c_a(w)(1+\omega)^4}{6c_a(\omega)(1+\omega)^{9/2}-2a_a(\omega)(1+\omega)^{1/2}}, \tag{46}$$

and

$$e_a(\omega)=\frac{\lambda_a^\infty\omega^2}{g(0)(1+\omega^4)}+\frac{\zeta_a}{6[\zeta_a-g(0)](1+\omega^4)}. \tag{47}$$

3. $G_n(q,i\omega)$

Finally, the local-field factor associated with number renormalisation of the Lindhard function is parametrized as

$$G_n(q,i\omega)=\frac{a_n(\omega)q+b_n(\omega)q^7}{1+c_n(\omega)q+d_n(\omega)q^6}, \tag{48}$$

where

$$a_n(\omega)=\frac{\lambda_n^0+\omega^2\lambda_n^\infty}{1+\omega^2}, \tag{49}$$

$$b_n(\omega)=-\frac{\lambda_n^\infty d_n(\omega)}{3}, \tag{50}$$

$$c_n(\omega)=\frac{a_n(\omega)}{2\lambda_n^\infty d_n(\omega)(1+0.38\omega)^{7/2}}-\frac{15a_n(\omega)+7\lambda_n^\infty}{6\lambda_n^\infty(1+0.38\omega)^{1/2}}-\frac{d_n(\omega)}{6}(1+0.38\omega)^{5/2}, \tag{51}$$

and

$$d_n(\omega)=\frac{\zeta_n}{(5\zeta_n+2\lambda_n^\infty)(1+\omega^4)}+\frac{\gamma_n\omega^{9/2}}{[5\gamma_n\omega^{1/2}+2\lambda_n^\infty(1+0.38)^{1/2}](1+0.38\omega)^3(1+\omega^4)}. \tag{52}$$

Here γ_n is determined by the peak height at large ω, i.e.,

$$\gamma_n=1.304r_s\frac{d}{dr_s}[r_s\epsilon_c(r_s)]. \tag{53}$$

These expressions for the local field factors, though cumbersome, are straightforward to evaluate and they require input of various quantities that we can readily obtain from QMC and other studies of the homogeneous two-dimensional electron gas. The correlation energy can be obtained from the diffusion Monte Carlo simulations of Rapisarda and Senatore.[16] For the pair correlation function we use the recently proposed expression[25]

$$g(0)=\frac{0.5}{1+1.372r_s+0.0830r_s^2} \tag{54}$$

that interpolates between the results of analytical studies at high densities and near Wigner crystallization. In addition, the spin susceptibility sum rule Eq. (21) can approximated by the following parametrization, namely,

$$\lambda_a^0(r_s)+\lambda_n^0(r_s)=\frac{2}{\pi+1.4954r_s+0.3193r_s^{1/2}}, \tag{55}$$

which is based on an extrapolation of available QMC data.[26] Finally, the structure factors appearing in Eq. (26) can be

TABLE I. Evaluation of r_s-dependent parameters as used in parametrized local-field factor expressions, Eq. (37), Eq. (42), and Eq. (48). Note that most of these values depend on the QMC calculations of the correlation energy and structure factors as reported in Ref. 16 and Ref. 27, respectively.

r_s	$g(0)$	λ_s^0	λ_s^∞	λ_a^0	λ_a^∞	λ_n^0	λ_n^∞	γ_n
1	0.2037	0.6907	0.3889	0.4324	0.2640	−0.0288	−0.3011	−0.1851
2	0.1227	0.7284	0.3889	0.3375	0.3301	−0.0338	−0.3622	−0.2227
5	0.0503	0.7998	0.4570	0.2059	0.4008	−0.0294	−0.3659	−0.2249
10	0.0217	0.8632	0.5424	0.1256	0.2271	−0.0209	−0.3211	−0.1968

obtained from the Fourier transforms of the two-dimensional spin-resolved pair correlation functions,

$$\tilde{S}(k)-1=\frac{n}{2}\int d^2r[g_{\uparrow\uparrow}(r)-g_{\uparrow\downarrow}(r)]\exp(-i\mathbf{k}\cdot\mathbf{r}), \quad (56)$$

and

$$S(k)-1=\frac{n}{2}\int d^2r[g_{\uparrow\uparrow}(r)+g_{\uparrow\downarrow}(r)-2]\exp(-i\mathbf{k}\cdot\mathbf{r}). \quad (57)$$

We obtain values of $g(r)$ at various values of r_s from very recent QMC studies[27] thereby enabling us to evaluate $\lambda_a^\infty(r_s)$ as given by Eq. (26). We report our results, along with all the other r_s-dependent parameters, in Table I.

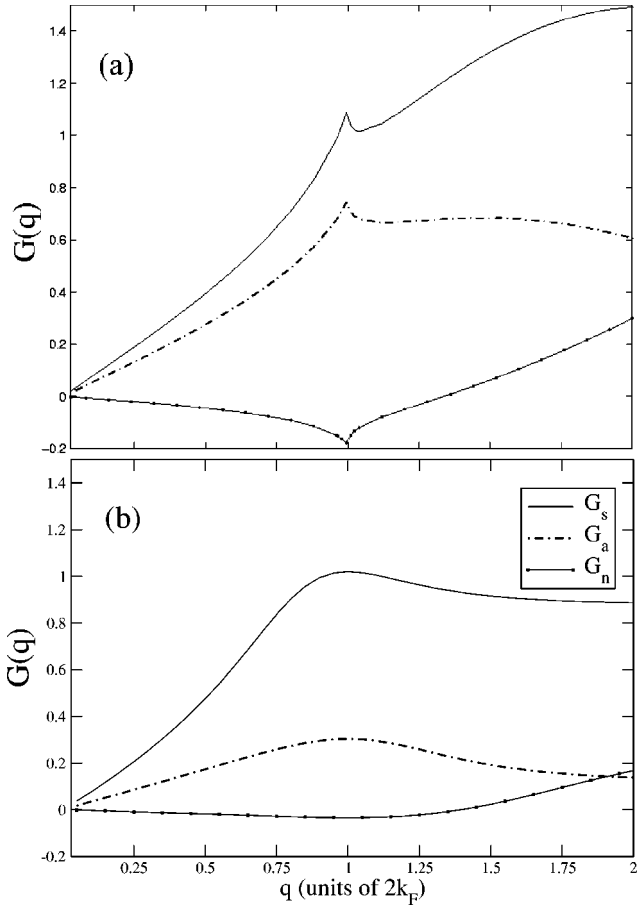

FIG. 2. Static local-field factors at $r_s=1$. (a) Evaluation from perturbation theory, Eqs. (16)–(18). (b) Evaluation from parametrized expressions, Eq. (37), Eq. (42), and Eq. (48).

The static local-field factors at $r_s=1$, as calculated by both the parametrized forms and by perturbation theory, are plotted in Fig. 2. The differences at large q highlight the failure of perturbation theory to satisfy the large-q sum rules. A comparison of the static and dynamic local-field factors is shown in Fig. 3 at $r_s=5$, and we collate some data in Table II for referential purposes in any future implementation of our parametrized scheme.

The static combinations of local-field factors Eq. (4) are shown in Fig. 4 and Fig. 5 and are compared with available data from QMC studies[27] at r_s values of 1, 2, 5, and 10. The generally favorable comparison demonstrates that the proposed parametrized expressions do capture most of the essential aspects of electron correlation to a very good degree, especially in the spin-antisymmetric case up to values of $q=1$ (i.e., $2k_F$). At higher values of q the parametrized expressions are strongly dependent on $g(0)$ and the deviation of the Monte Carlo data at this regime suggests that the fitting formula for $g(0)$ proposed in Ref. 28 as given by Eq. (54), overestimates the results of QMC simulations for most densities in the regime $1\leqslant r_s\leqslant 10$. This conclusion concerning Eq. (54) has also very recently been pointed out in the work of Bulutay and Tanatar.[29] In general, it can be gleaned from the figures that the perturbation scheme employed in Sec. II A, which determines the structure at low q, is quite accurate for the spin-antisymmetric case (Fig. 5) but less so for the spin-symmetric case (Fig. 4). The structure predicted by the perturbative calculations, in particular the maxima at $q=1$, appears to be somewhat washed out in the spin-symmetric QMC results for low r_s or is shifted to higher

TABLE II. Calculated values of the parametrized local-field factors at $r_s=5$.

ω	q	$G_s(q,i\omega)$	$G_a(q,i\omega)$	$G_n(q,i\omega)$
0	0.5	0.522	0.106	−0.016
0	1.0	1.120	0.185	−0.029
0	1.5	0.997	0.105	0.023
0.5	0.5	0.414	0.082	−0.030
0.5	1.0	0.939	0.500	−0.066
0.5	1.5	0.970	0.049	−0.001
1.0	0.5	0.349	0.151	−0.093
1.0	1.0	0.854	0.056	−0.165
1.0	1.5	0.967	0.050	−0.132

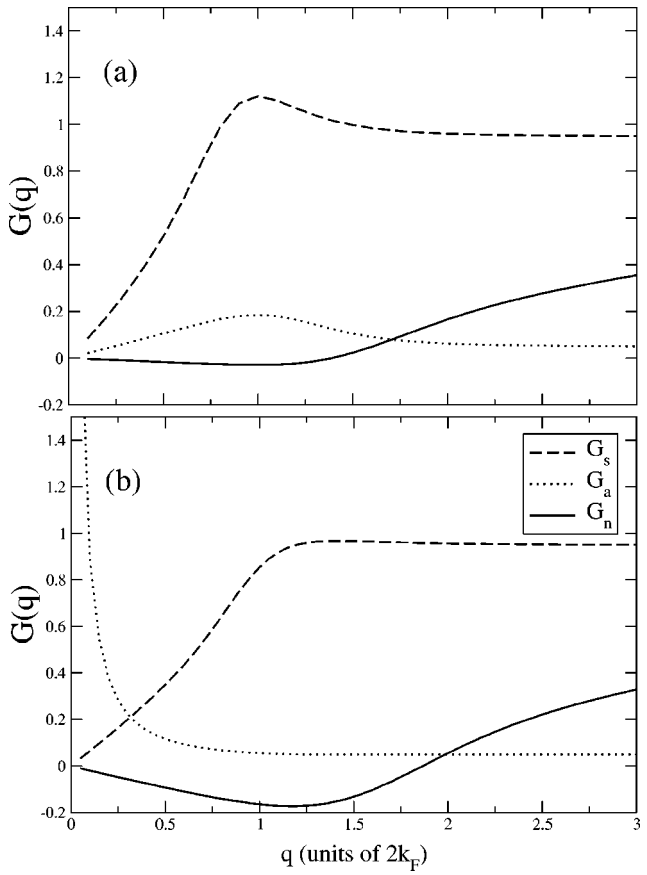

FIG. 3. Parametrized local-field factors from Eq. (37), Eq. (42), and Eq. (48) at $r_s=5$. (a) Static ($\omega=0$). (b) Dynamic ($\omega=1$).

values of q as in the case of $r_s=10$. This suggests that, at least in two dimensions, the higher-order diagrams excluded from Fig. 1 may play a significant role in calculations of the charge-density response, but are not important to calculations for the spin-density response because of mutual cancellations amongst the diagrams. We speculate on the nature of these cancellations in Sec. IV.

There exists, at present, no corresponding dynamical QMC studies of electrons in two dimensions and thus the efficacy of the parametrized local field factors at finite frequencies remains to be tested directly.

III. EFFECTIVE ELECTRON-ELECTRON INTERACTIONS

With the many-body effects encaptured by the local-field factors it is now possible to determine the effective interaction between two electrons in a fully interacting sea of electrons that rearrange themselves because of screening, exchange, and other correlation effects. We use the expression for the effective electron-electron interaction as proposed by KO, namely,

$$V^{\mathrm{eff}}_{\sigma\sigma'}=\Lambda^2(\tilde{q})\frac{v_q}{\epsilon(\tilde{q})}+\frac{[v_qG_s(\tilde{q})]^2\overline{\Pi}_0(\tilde{q})}{1+v_qG_s(\tilde{q})\overline{\Pi}_0(\tilde{q})}+\sigma\sigma'\frac{[v_qG_a(\tilde{q})]^2\overline{\Pi}_0(\tilde{q})}{1+v_qG_a(\tilde{q})\overline{\Pi}_0(\tilde{q})}, \tag{58}$$

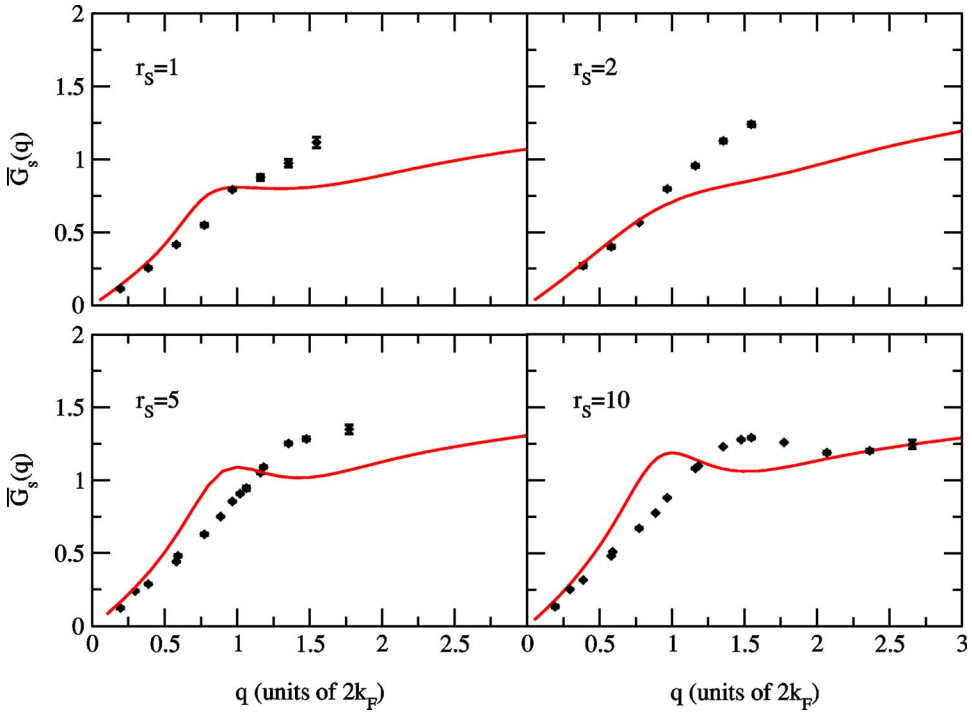

FIG. 4. Spin-symmetric local-field factors. The continuous lines are evaluated from the parametrized expressions, Eq. (37) and Eq. (48), and the individual data points are from QMC calculations (Ref. 27).

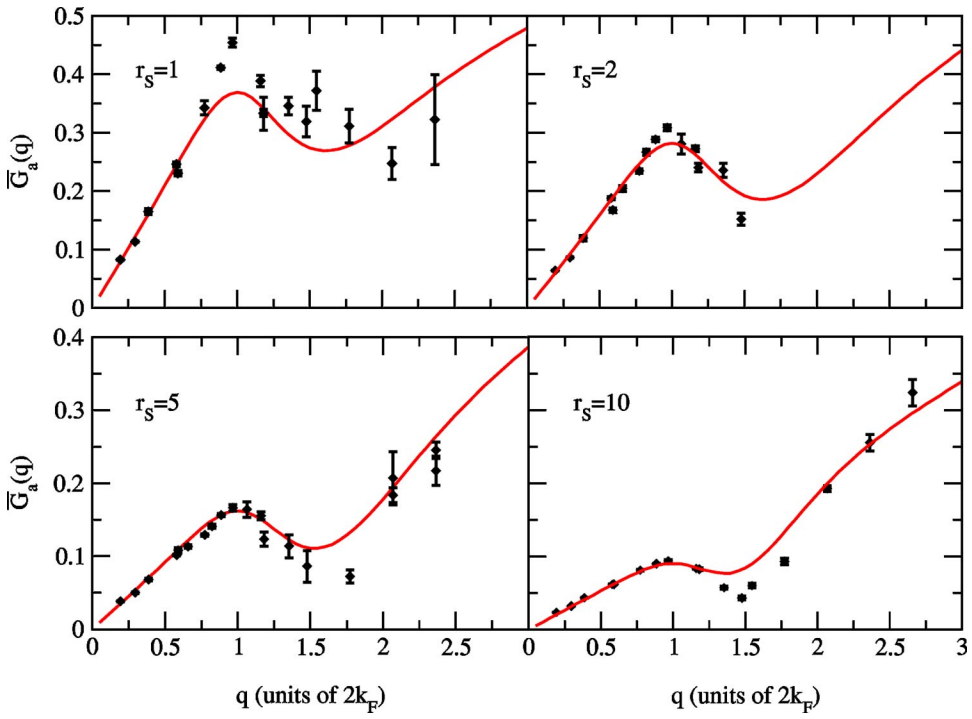

FIG. 5. Spin-antisymmetric local-field factors. The continuous lines are evaluated from the parametrized expressions, Eq. (42) and Eq. (48), and the individual data points are from QMC calculations (Ref. 27).

where $\Lambda(\tilde{q})$ is the vertex function,

$$\Lambda(\tilde{q}) = \frac{1}{1+v_q G_s(\tilde{q})\overline{\Pi}_0(\tilde{q})}, \tag{59}$$

σ are the Pauli spin matrices, and $\epsilon(\tilde{q})$ is the dielectric function,

$$\epsilon(\tilde{q}) = 1 - v_q \overline{\Pi}_0(\tilde{q})\Lambda(\tilde{q}). \tag{60}$$

The KO expression neglects the contribution of transverse spin fluctuations[30] and thus represents a strictly local approximation. The static effective electron-electron interaction using the parametrized local-field factors is shown in Fig. 6 for triplet pairing. As previously shown,[8] the singular nature at $q=1$ (i.e., $2k_F$) is more pronounced in two dimensions than in three[4] and is also reflected in an *attractive* interaction for triplet pairing at lower densities. Approximations that neglect the peaked structure at $q=1$ do not give rise to attractive regions of the interelectron potential.

The frequency-dependent effective electron-electron interaction is shown in Fig. 7 at various values of r_s. The nonmonotonic deviation from the static approximation ($\omega=0$) is quite evident and, as expected, the non-negligible frequency dependence increases with correlation, i.e., r_s.

IV. DISCUSSION AND CONCLUSIONS

In summary, we have determined parametrized expressions for the two-dimensional dynamical local-field factors based on all available sum rules and diagrammatic summation of classes of diagrams. The parametrized expressions, which have no further adjustable constants, have been shown to compare well with (static) QMC simulations, particularly in the spin-antisymmetric case. Finally, the effective two-dimensional electron-electron interaction has been evaluated using the parametrized local-field factors within the KO local approximation.

The agreement of the spin-antisymmetric local-field factor with the QMC results, at intermediate wave vectors, is particularly notable given that perturbation theory, and not exact sum rules, has been used to determine the peak heights at $q=1$. This, fortuitously, suggests that higher-order diagrams are mutually cancelled to a large degree even though the individual diagrams may themselves have large contribu-

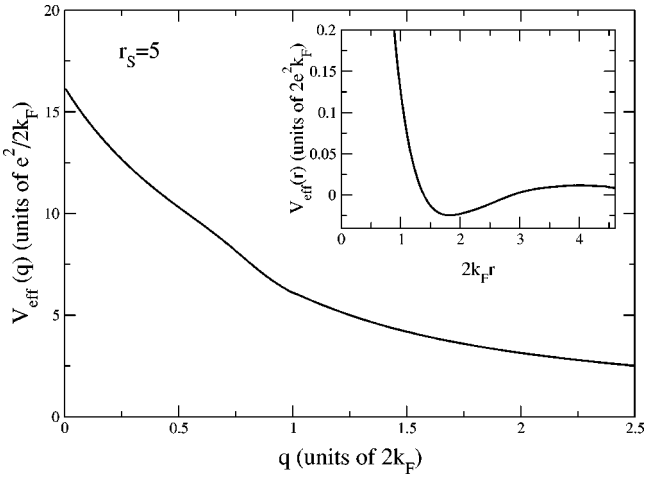

FIG. 6. Static effective electron-electron potential at $r_s=5$. The inset shows the real-space behavior.

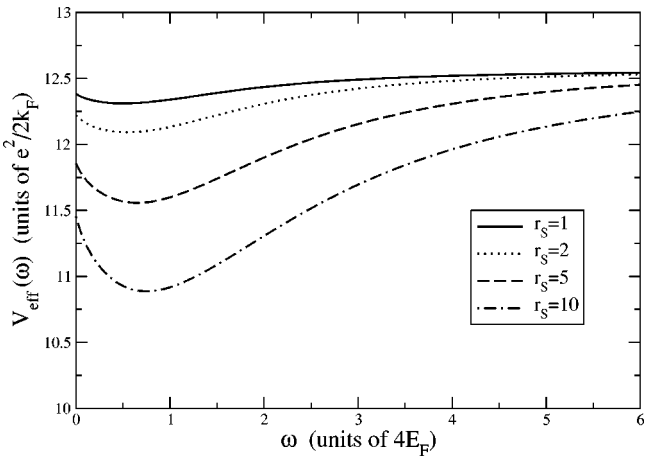

FIG. 7. Dynamical effective electron-electron interaction at $q=0.5$ as a function of imaginary frequency.

tions. There are two possible reasons for this cancellation: (i) summation of terms alternating in spin (sign) and (ii) self-consistent cancellation of self-energy and vertex corrections attributable to gauge invariance (i.e., Ward identities). Explicit evaluation of higher-order diagrams will be needed to assess these conjectures.

However, the case of the spin-symmetric local-field factor is less satisfactory at $q=1$, probably because of the lack of cancellation between spin-up and spin-down contributions. The singular peaks at $q=1$ found in perturbation theory do not appear convincingly in the QMC data: it is either washed out or, surprisingly, shifted to higher wave vectors. With only one set of such data available we have to await further, and more accurate, QMC calculations, which are currently being carried out[27] before we can make any definitive conclusions.

The $\mathbf{q}$ and ω dependences of the local-field factors are a reflection of the spatial and temporal nonlocality of the xc kernel $K_{xc}(\mathbf{r},t;\mathbf{r}',t')$ in time-dependent density-functional theory. Lein *et al.*[31] have investigated the importance of such dependences from various approximate forms of three-dimensional local-field factors and concluded that, in determining the correlation energy, the momentum dependence cannot be neglected, while the frequency dependence, though significant, is less important. Physically, this implies that, at least for correlation energy calculational purposes, it is necessary to acknowledge the spatial extent of xc hole, whilst the retarded nature of the dynamics can be neglected, i.e., through use of the adiabatic approximation. In two dimensions correlation effects on the $\mathbf{q}$ dependence are greater,[32,33] as demonstrated by the singular peak in the polarizability at $q=1$. In addition, the gapless nature of the two-dimensional plasmon requires that the characteristic charge-density response time goes to infinity in the long wavelength limit, and hence the adiabatic approximation (i.e., neglect of ω dependence) is expected to be even less satisfactory in two dimensions than in three.[34] In summary, the case of two dimensions is interestingly different from that of three dimensions in that the $(\mathbf{q},\omega)$ dependences of correlation effects are enhanced for a given r_s. Hence, it would be useful to carry out a similar calculation of the correlation energy to explicitly verify the increasing importance of dynamical correlation in two dimensions.

It is worth emphasizing that the results reported here apply strictly to a single-band system. Multiband systems, in particular compensated electron-hole systems, permit the possibility of correlated charge fluctuations between the bands. Previous work[35] on three-dimensional systems has demonstrated that the two-band case has a strikingly different effect on the effective electron-electron interaction, where an additional *attractive* term arises precisely from these charge fluctuations. This reflects an enhancement of the underlying local-field effects which we expect to occur also, if not to a greater extent, in compensated two-dimensional electron-hole systems.

Finally, we note that an intriguing application of the dynamical local-field factors is in the effective electron-electron interaction where correlation effects may be giving rise to regions of attraction, and thus possibly mediating intrinsic superconducting instabilities.[36] Preliminary numerical solutions of the Eliashberg gap equation have been carried out,[37] indicating that electronic dynamical correlation raises the intrinsic pairing transition temperature as the dimensionality of the isotropic electron liquid is lowered from three to two.

ACKNOWLEDGMENTS

We are grateful to Dr. Saverio Moroni for sharing his results of QMC calculations, of which only some have been published earlier.[38] This work was supported by the NSF under Grant No. DMR-9988576.

[1] J. Hubbard, Proc. R. Soc. London, Ser. A **240**, 539 (1957).
[2] N. Iwamoto, Phys. Rev. A **30**, 3289 (1984).
[3] J. Lindhard, K. Dan. Vidensk. Selsk. Mat. Fys. Medd. **28**, 8 (1954).
[4] C.F. Richardson and N.W. Ashcroft, Phys. Rev. B **50**, 8170 (1994).
[5] K.S. Singwi, M.P. Tosi, R.H. Land, and A. Sjolander, Phys. Rev. **176**, 589 (1968).
[6] D.J.W. Geldart, Can. J. Phys. **45**, 3139 (1967).
[7] C.A. Kukkonen and A.W. Overhauser, Phys. Rev. B **20**, 550 (1979).
[8] I.G. Khalil, M. Teter, and N.W. Ashcroft, Phys. Rev. B **65**, 195309 (2002).
[9] S.S. Jha, K.K. Gupta, and J.W.F. Woo, Phys. Rev. B **4**, 1005 (1971).
[10] D.J.W. Geldart and S.H. Vosko, Can. J. Phys. **44**, 2137 (1966).
[11] G.S. Atwal and N.W. Ashcroft, Phys. Rev. B **65**, 115109 (2002).
[12] R. Cenni and P. Saracco, Nucl. Phys. A **487**, 279 (1988).
[13] R. Cenni and P. Saracco, Riv. Nuovo Cimento **15**, 12 (1992).
[14] A. Neumayr and W. Metzner, Phys. Rev. B **58**, 15 449 (1998).
[15] I. G. Khalil, Ph.D. thesis, Cornell University, 2001.
[16] F. Rapisarda and G. Senatore, Aust. J. Phys. **49**, 161 (1996).

[17] Z. Qian and G. Vignale, Phys. Rev. B **65**, 235121 (2002).
[18] S. Conti and G. Vignale, Phys. Rev. B **60**, 7966 (1999).
[19] Y. Kwon, D.M. Ceperley, and R.M. Martin, Phys. Rev. B **50**, 1684 (1994).
[20] B. Goodman and A. Sjolander, Phys. Rev. B **8**, 200 (1973).
[21] G. S. Atwal and N. W. Ashcroft, (unpublished).
[22] G. Santoro and G. Giuliani, Phys. Rev. B **37**, 4813 (1988).
[23] G. Niklasson, Phys. Rev. B **10**, 3052 (1974).
[24] X. Zhu and A.W. Overhauser, Phys. Rev. B **30**, 3158 (1984).
[25] B. Davoudi, M. Polini, G.F. Giuliani, and M.P. Tosi, Phys. Rev. B **64**, 233110 (2001).
[26] B. Davoudi, M. Polini, G.F. Giuliani, and M.P. Tosi, Phys. Rev. B **64**, 153101 (2001).
[27] S. Moroni (private communication).
[28] M. Polini, G. Sica, B. Davoudi, and M.P. Tosi, J. Phys.: Condens. Matter **13**, 3951 (2001).
[29] C. Bulutay and B. Tanatar, Phys. Rev. B **65**, 195116 (2002).
[30] G. Vignale and K.S. Singwi, Phys. Rev. B **32**, 2156 (1985).
[31] M. Lein, E.K.U. Gross, and J.P. Perdew, Phys. Rev. B **61**, 13 431 (2000).
[32] M. Jonson, J. Phys. C **9**, 3055 (1976).
[33] A. Czachor, A. Holas, S.R. Sharma, and K.S. Singwi, Phys. Rev. B **25**, 2144 (1982).
[34] K. Takayanagi and E. Lipparini, Phys. Rev. B **54**, 8122 (1996).
[35] C.F. Richardson and N.W. Ashcroft, Phys. Rev. B **55**, 15 130 (1997).
[36] W. Kohn and J.M. Luttinger, Phys. Rev. Lett. **15**, 524 (1965).
[37] G. S. Atwal, Ph.D. thesis, Cornell University, 2002.
[38] *Quantum Monte Carlo Methods in Physics and Chemistry*, edited by M. P. Nightingale and C. J. Umrigar, (Kluwer, Dordrecht, 1999).